N 69 39296
NASA CR 106233

TERRAIN MODELING FOR SURFACE VEHICLE GUIDANCE

R.J. Mancini

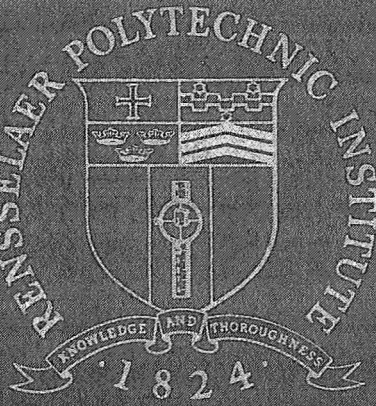

Rensselaer Polytechnic Institute
Troy, New York

R.P.I. Technical Report MP-11

TERRAIN MODELING FOR SURFACE VEHICLE GUIDANCE

R.J. Mancini

NASA Grant NGL 33-018-091

Analysis and Design of a Capsule Landing System
and Surface Vehicle Control System for Mars Exploration

AUGUST 1969

Rensselaer Polytechnic Institute
Troy, New York

ABSTRACT

The problem considered was the development of methods to mathematically model major terrain features for an autonomous surface vehicle guidance system. The terrain information available was restricted to data that could be measured by the vehicle's terrain sensor, which was assumed to provide range readings for specified values of azimuth and elevation angles.

Terrain indices were developed to process the sensor measurements. The purpose of these indices is to enable the vehicle to directly or indirectly detect major terrain features that represent an obstacle to travel. Modeling methods were then constructed from the indices to provide a systematic means of modeling the terrain.

Simulated sensor measurements were obtained by using the geodetic survey map of a relatively hilly portion of terrain. The simulated sensor data was then used to evaluate the effectiveness of the modeling methods. The effectiveness of a particular method was primarily defined in terms of the percentage of passable terrain that could be detected and the error in range due to overestimating the distance to a terrain obstacle.

It is concluded that it is feasible to model major terrain features for a vehicle guidance system with only a modest onboard computer requirement. Three alternative modeling methods were developed that are applicable to relatively rough terrain.

The method chosen for a particular situation would depend on the modeling effectiveness desired and the sensor and computer capability available.

TABLE OF CONTENTS

LIST OF ILLUSTRATIONS

LIST OF TABLES

List of Tables (Cont'd....)

LIST OF SYMBOLS

R	measured range to a point on a terrain feature
θ	azimuth direction to a point on a terrain feature
$\Delta\theta$	discrete change in θ
β	elevation angle to a point on a terrain feature
$\Delta\beta$	discrete change in β
Z	relative altitude of terrain with respect to the vehicle
D	horizontal distance from the vehicle
G	gradient of a terrain feature
S_I	in-path slope
S_c	cross-path slope
T_s	slope index test number
T_g	gradient index test number
T_r	relative altitude index test number
T_v	vertical index test number
T_d	discontinuity index test number

ACKNOWLEDGMENT

The author would like to express his gratitude to Professor D.K. Frederick for his supervision of this research and to Professor S.W. Yerazunis and Mr. E. Suggs for their timely and helpful suggestions.

This research was supported by the National Aeronautics and Space Administration under Research Grant NGL 33-018-091, for which support the author is very grateful.

I. INTRODUCTION

The problem under consideration is the mathematical modeling of major terrain features using line-of-sight sensor measurements acquired from a single terrain location. This investigation is part of an overall National Aeronautics and Space Administration sponsored study of a surface vehicle control system for the unmanned exploration of Mars. It is assumed that the exploration vehicle will have to travel a considerable distance, perhaps a hundred kilometers or more, from its initial landing site to one or more remote locations to complete its mission. The vehicle is considered to be operating independent of Earth-based control or other orbiting satellites. Thus, the guidance system must be self-contained, and it must be capable of processing terrain information and making a path selection decision.

The path selected should not only lead the vehicle toward its objective, but also should provide a safe path of travel for the vehicle. If the vehicle should encounter a terrain hazard, the mission could end in failure. Thus, the guidance system must be able to: 1). avoid short range obstacles that represent an immediate danger to the safety of the vehicle, and 2). select a long range path around major terrain features that obstruct a direct and safe route to the objective. This report deals specifically with the terrain model required to perform long range path selection.

A number of path selection algorithms (Ref. 1,2) have been developed which can be used for long range vehicle guidance. In order to utilize these algorithms, however, the terrain must be modeled with respect to the obstacles that are in the vicinity of the vehicle location. The terrain model required is two dimensional in nature and simply describes the distance a vehicle can travel before encountering an obstacle in a series of discrete azimuth directions. A sample terrain model is pictorial represented in Figure 1.

Basically, there are three main steps that must be performed by a terrain modeling system, namely:

a) Terrain Data Acquisition

b) Terrain Data Processing

c) Terrain Model Generation

Section II deals specifically with terrain data acquisition. Since specifications of a sensor to acquire terrain data have not been defined, typical long range sensor measurements are simulated to indirectly determine some general sensor measurement characteristics. The sensor data simulation is performed by assuming various vehicle locations on a geodetic map, and then converting topographic information into sensor data, i.e., range measurements for specified values of azimuth and elevation angles.

In Section III, a number of indices are developed to process the sensor terrain data in order to detect the presence of a terrain obstacle. The terrain indices are combined in

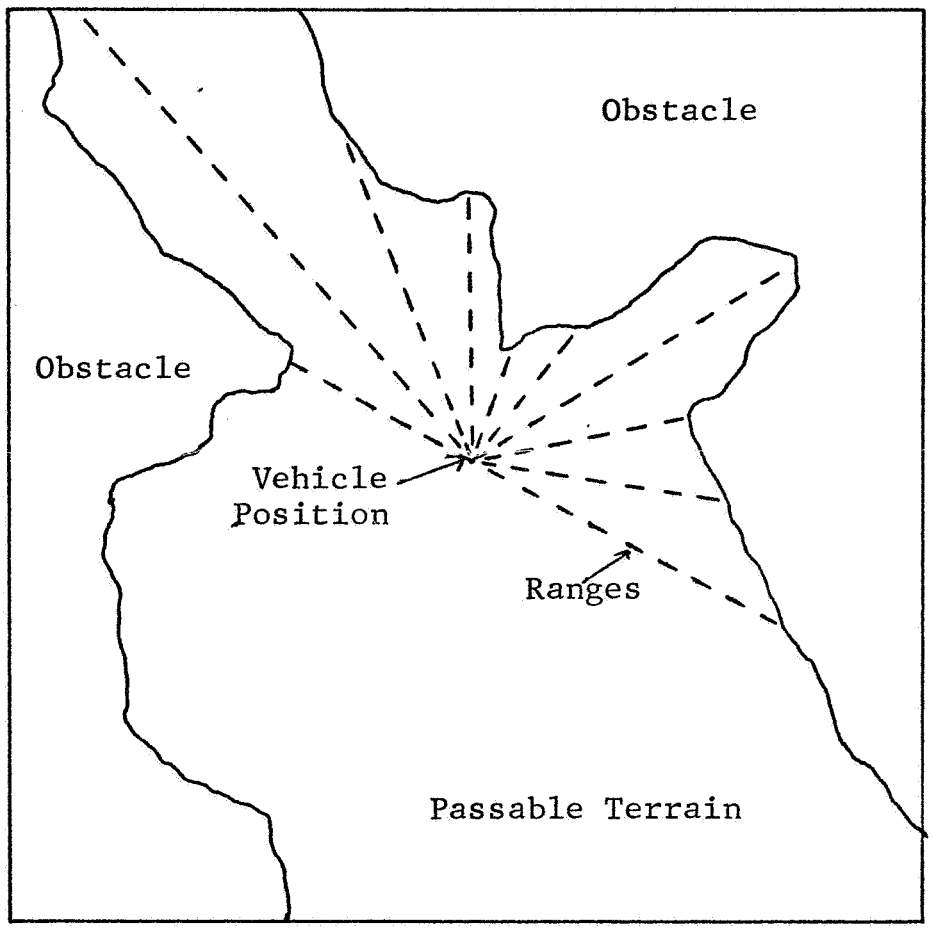

FIGURE 1. Terrain Model

Section IV to provide several systematic methods to generate a terrain model. The simulated sensor data is then used to evaluate the effectivenss of the modeling methods. The effectiveness of a method is primarily defined in terms of the percentage of passable terrain that can be detected and the error in range due to overestimating the distance to a terrain obstacle. Then, some general sensor measurement requirements are described in terms of the effectiveness of the modeling methods.

II. TERRAIN SIMULATION

A. Sample Terrain

There are four general terrain characteristics that significantly effect a vehicle's performance (Ref. 3,4,5). These characteristics are:

a) surface composition

b) surface geometry

c) vegatation structure

d) hydrologic geometry

Presently, there is relatively little known about the surface conditions on Mars. From the general information that is available, there is no evidence of vegatation or significant amounts of water present. The surface composition is a matter of speculation. Considering the surface geometry, it is estimated (Ref. 6) that slopes of major terrain features generally vary between 0 and 30 degrees, and that over half of the slopes are less than 10 degrees.

Thus, the surface geometry is the only terrain characteristic which will be considered in this study as constituting an obstacle to travel.

For the purposes of long range terrain modeling, a slope of a major terrain feature equal to or greater than 10 degrees will be defined as an obstacle. Slope, in its classical sense, is defined as the angular deviation of a surface from the horizontal, measured perpendicular to the topographic contours. Slope so defined can be measured from a contour map. A major terrain feature is defined as an area that is significantly larger than the dimensions of the exploratory vehicle (Ref. 7). The 10 degree slope, as the definition of an obstacle, was somewhat arbitrarily chosen, and it may even be considered conservative with respect to the climbing capabilities of proposed exploratory vehicles. In justification of this obstacle definition, it should be kept in mind that an exploratory vehicle may encounter adverse soil conditions or some unknown element that could substantially reduce the vehicle's climbing capabilities.

Slope was the only surface geometry factor considered as a true obstacle. Such factors (Ref. 4,8,9,10) as slope segments, spacing and size of vertical obstacles, terrain approach angles, etc. are pertinent to short range terrain modeling and will not be discussed further.

A geodetic map (Ref. 11) was used to represent a sample terrain and was the source of empirical terrain data for the terrain modeling techniques developed. The map selected represented a section of hilly terrain near the Catskill region in New York State with a scale of 1:24000 and a contour interval of 10 feet. The slopes of major terrain features varied between 0 and 30 degrees, whereas the slopes of typically encountered terrain features varied between 0 and 15 degrees. This slope variation is somewhat comparable to the values for Mars referred to earlier.

Several significantly different geometrical terrain configurations were specifically analyzed in detail in the hope that the results of this investigation would be applicable to a variety of terrain situations. The three areas selected are listed below with a brief description of their salient features, as seen from the assumed positions of the vehicle. The sectors are indicated in Figures 2 and 3.

Area 1: The vehicle's vantage point is on the summit of a hill (reference map grid coordinate 16420962*). The vehicle is sighting east across a valley toward a ridge line. A 35 degree sector of terrain was considered (see

* The first four digits refer to the east-west grid lines, and the last four digits refer to the north-south grid lines.

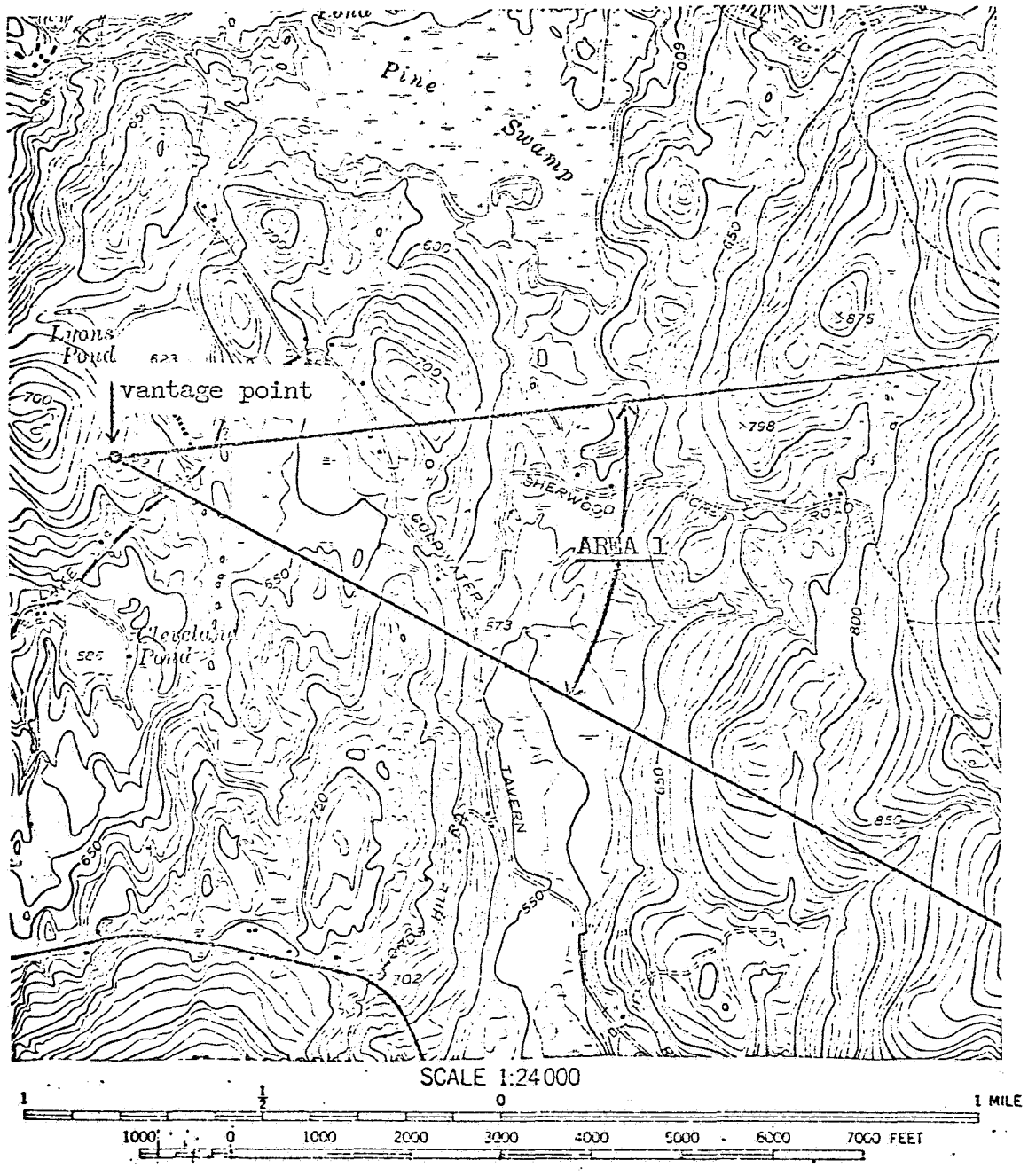

FIGURE 2. Area 1 of the Sample Terrain

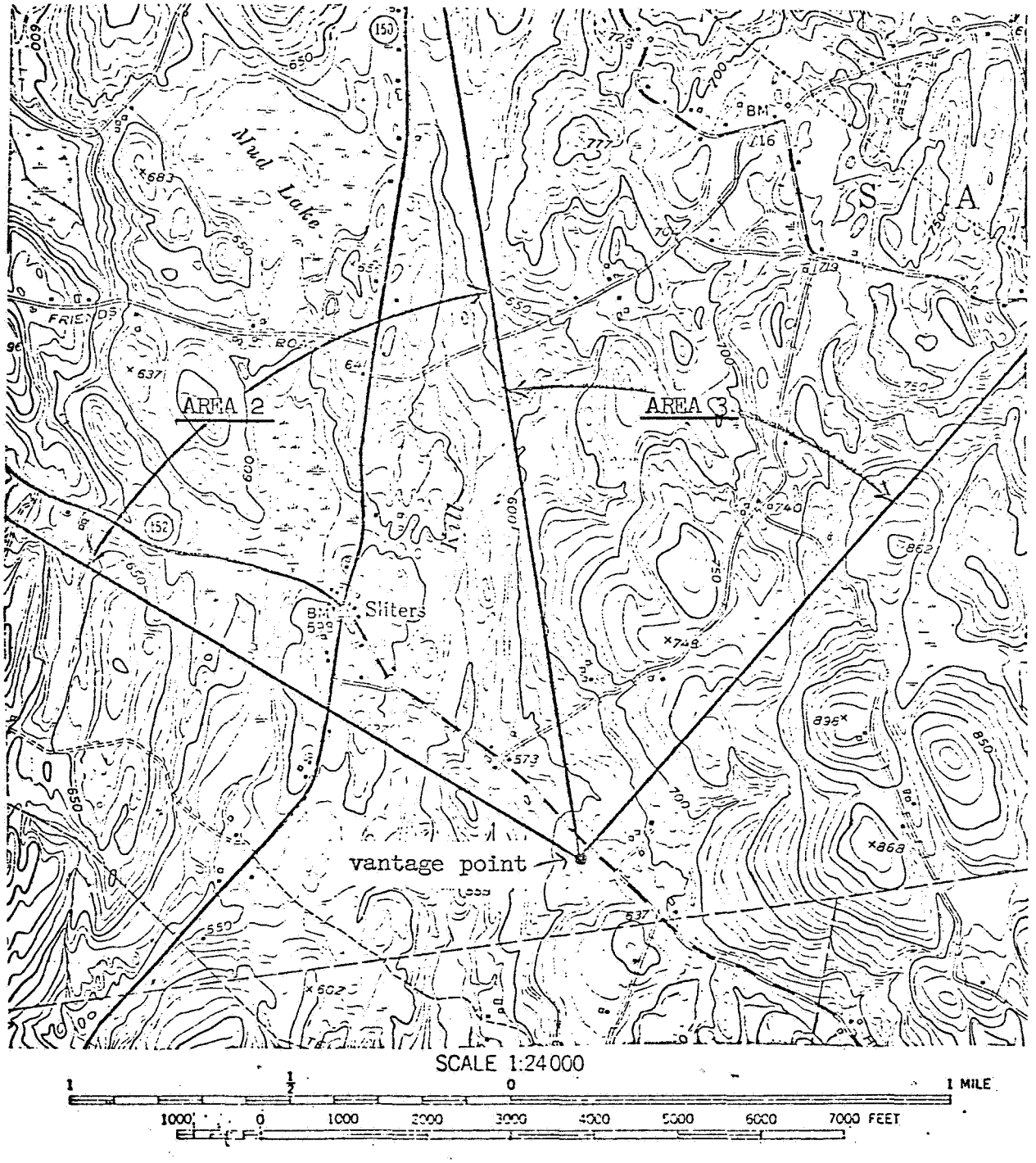

FIGURE 3. Areas 2 and 3 of the Sample Terrain

Figure 2).

Area 2: The vehicle's vantage point is on a gentle rise (reference map grid coordinate 14601673). The vehicle is sighting north-northwest toward relatively minor hills and valleys scattered through the area. A 50 degree sector of terrain was considered (see Figure 3).

Area 3: The vehicle's vantage point is on a gentle rise (reference map grid coordinate 14601673). The vehicle is sighting north-northwest toward a relatively high mountainous area. A 50 degree sector of terrain was considered (see Figure 3).

In addition to the areas described above, other selected profiles of terrain were also considered, such as from a valley location sighting across a flat area towards a mountainous region, and from the summit of a hill sighting toward a valley.

B. Terrain Data Acquisition

The acquisition of data by a terrain sensor on the vehicle was simulated by making measurements on the geodetic map in the areas decribed above.

Three types of sensor measurements, i.e., azimuth angle, elevation angle and range, are assumed to be available, from which all terrain information must be obtained. The azimuth angle (θ) represents the angle the terrain sensor is directed in the horizontal plane of the vehicle.

Angles of θ will be measured with reference to some convenient azimuth direction, e.g., grid north on the geodetic map is 0^{o}. The elevation angle (β) is the angle the sensor is directed in the vertical plane of the vehicle. Angles of β will be measured with reference to the horizontal plane at the vehicle's location, with angles above the horizontal considered positive. The range (R) is the distance the sensor can measure along the line of sight to a terrain feature. The angles θ and β are adjusted at the vehicle and thus are independent variables, whereas R is a dependent variable. It is assumed that values of R can only be measured at discrete increments of θ and β , and that the size of these discrete increments is a characteristic of the sensor which must be specified.

In order to simulate the terrain data which the vehicle would receive from a particular vantage point, values of distance and relative altitude (Z) were measured directly from the geodetic map for a fixed value of azimuth angle (θ). From this information, terrain profiles of altitude vs. distance plots were constructed for each value of θ as illustrated in Figure 4.

The procedure used to obtain simulated sensor data was to assume a sensor range measurement, R, to a point on the terrain profile. Then the corresponding elevation

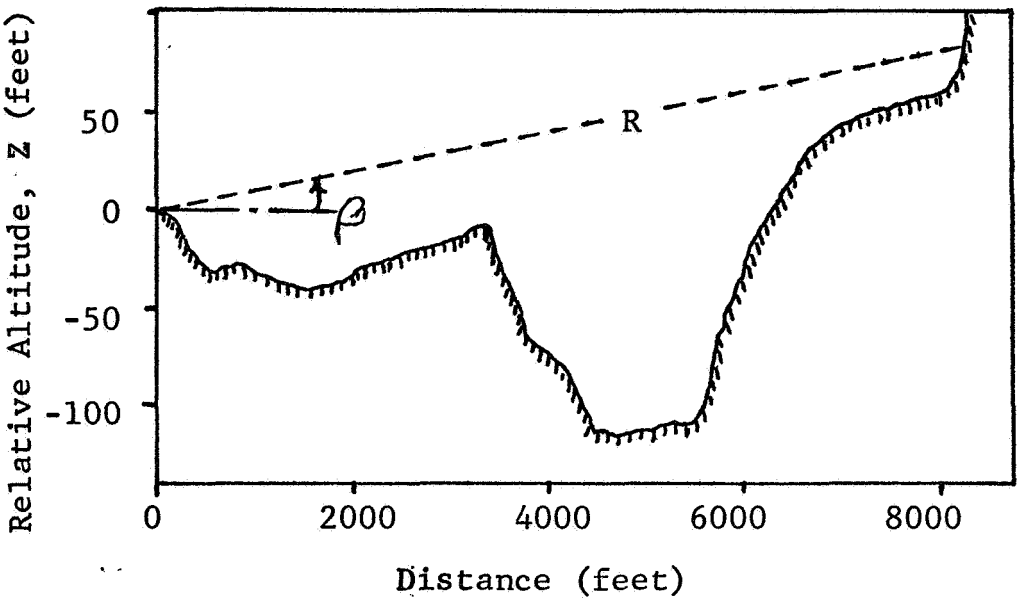

FIGURE 4. Terrain Profile

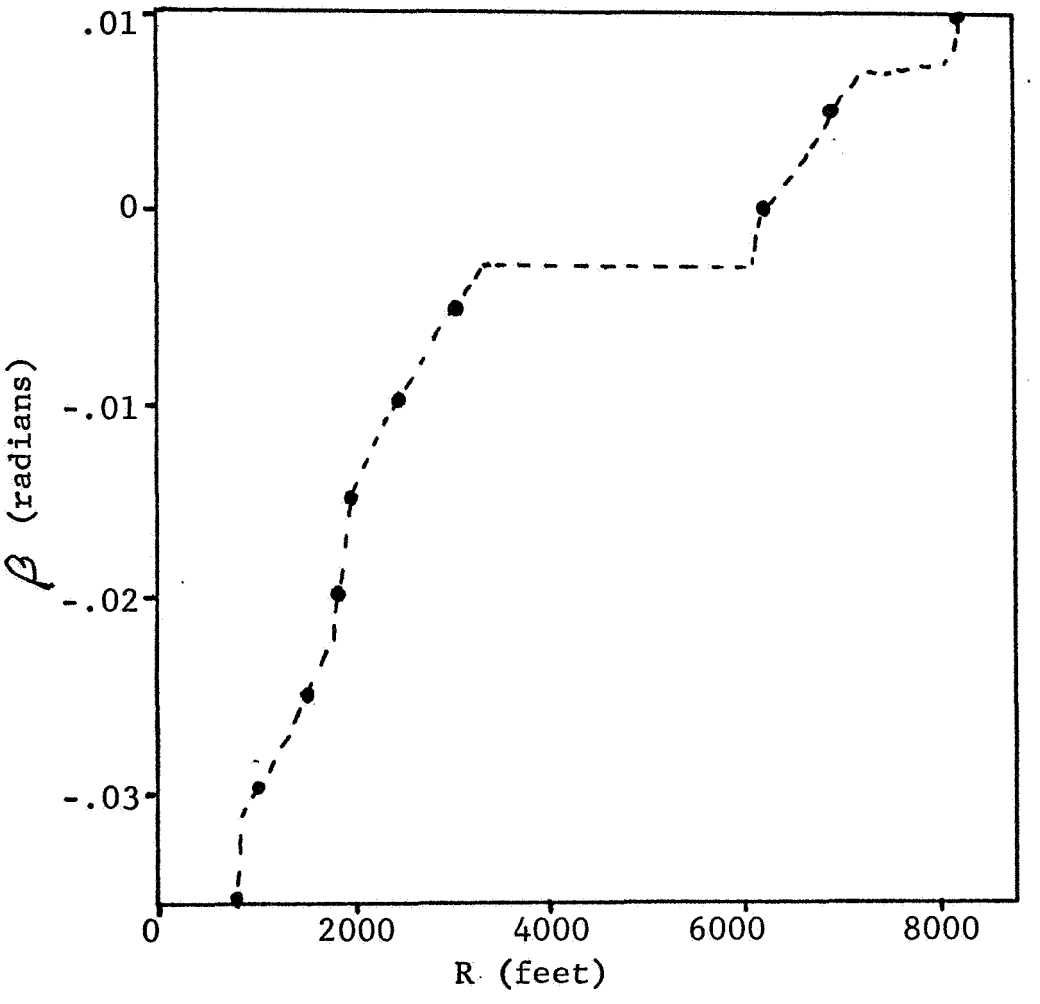

FIGURE 5. β vs. R Sensor Measurement Plot

angle, β, could be calculated from

$$\sin \beta = \frac{Z}{R} \tag{2.1}$$

Figure 5 is the corresponding β—R plot for the terrain profile presented in Figure 4. The points along the continuous β—R curve are the discrete sensor data the vehicle would receive in the absence of measurement errors. It is noted that if areas of the terrain profile were hidden from the vehicle's view, there would be a corresponding discontinuous horizontal segment on the β—R plot, as illustrated in Figures 4 and 5.

Sensor measurements were also compiled in the form of θ vs. R polar plots, with β held constant. The polar plot can be constructed from either the β—R plots taken in a series of azimuth directions or directly from the geodetic map using templates graduated in Z and R for fixed values of β. The θ—R polar plots are useful in detecting major terrain formations but are only indirectly related to the slopes of these terrain formations. Figure 6 is a θ-R polar plot acquired with β fixed at a small positive value. The areas labeled with a C were relatively clear of high terrain formations, i.e., no terrain feature was sensed in the ranges considered. Conversely, the areas labeled A,B,D and E corresponded to relatively high terrain formations.

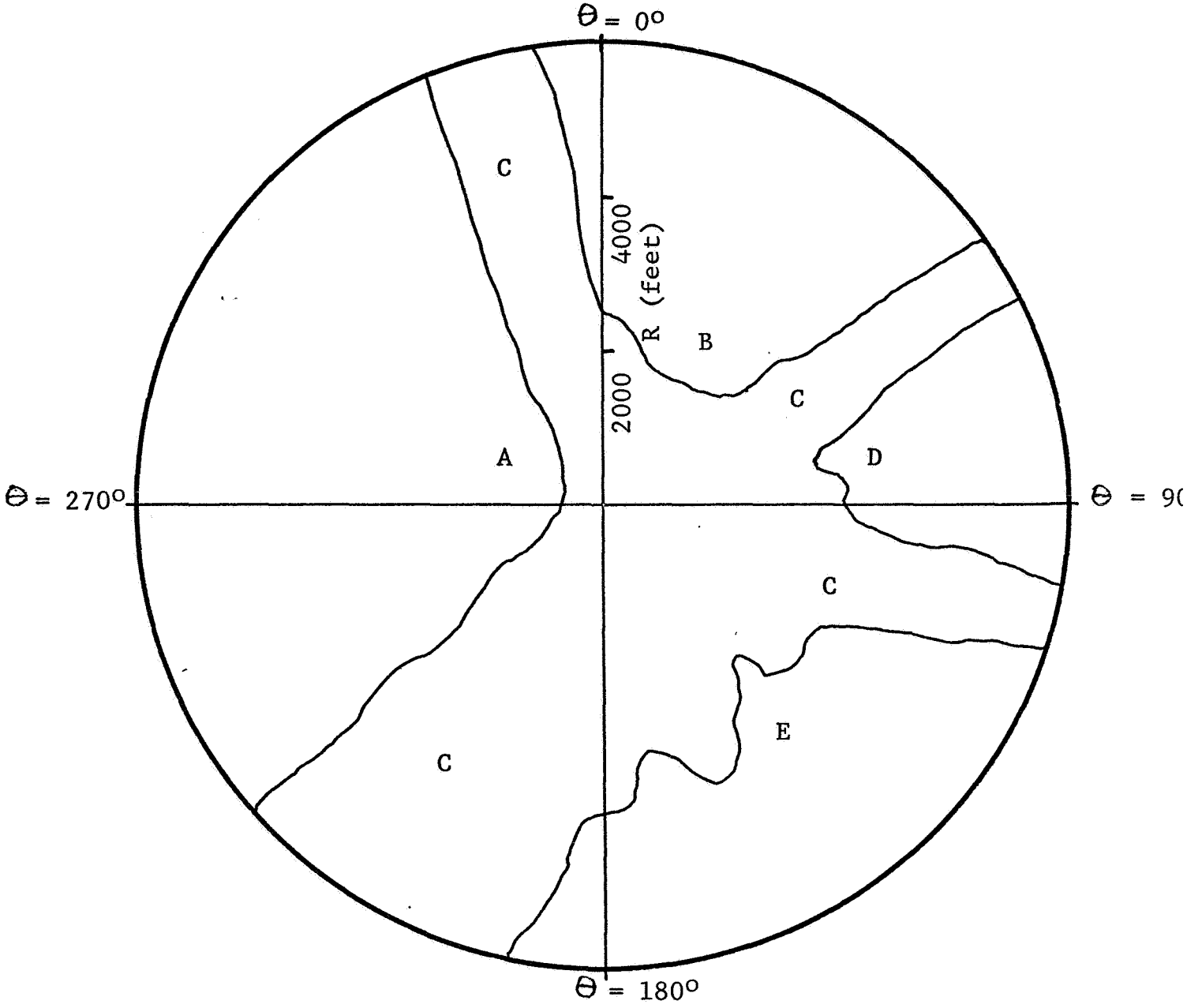

FIGURE 6. Θ vs. R Sensor Measurement Polar Plot

C. Characteristics of Sensor Measurements

Sensor measurements of the sample terrain were predominantly compiled in the form of β—R plots. These plots were found to be more useful than the Θ—R plots for analyzing the sensor data and developing terrain modeling techniques since they yielded information directly related to the slope of the terrain along a profile. The β—R plots were prepared in azimuth increments ($\Delta\Theta$) of 5 degrees for the areas of the map described above. A total of 35 such plots were drawn. Since the β—R plots were acquired from various types of terrain configurations, certain sensor measurement characteristics were deduced from the data.

A range of 400 feet from the vehicle was the minimum value for which useful empirical data could be obtained from the geodetic map due to the lack of sufficient contour information in the proximity of the assumed vehicle locations. The vehicle locations were specifically chosen so as not to be in areas of large contour variation since the purpose of the guidance system is to keep the vehicle away from such areas. Due to the lack of short range contour information, sensor measurements often had to be approximated when R was less than 400 feet. Thus, any conclusions drawn from the simulated terrain data only pertain to terrain at ranges greater than 400 feet from the vehicle.

The maximum feasible range for modeling the sample terrain was chosen as 4000 feet since there were insufficient sensor measurements available to the vehicle at greater range values. Figure 7 is a historgram of the number of sensor measurements acquired from 35 β—R plots ($\Delta\beta$ = .005 radian) as a function of the range at which the measurements were sensed. Nearly 90% of the discrete sensor measurements were sensed at ranges of less then 3500 feet.

The maximum value of β needed to acquire sensor information was .073 radian (4.2 degrees). Approximately 80% of the sensor measurements were acquired for values of $\beta = \pm .030$ radian (1.8 degrees). For all values of β encountered, small angle approximations were certainly valid. A typical use of this approximation was in the calculation of β from the terrain profile measurements using

$$\beta = \frac{Z}{R} \tag{2.2}$$

III. TERRAIN DATA PROCESSING

The terrain data in the form of a set of sensor measurements R_i, β_i and Θ_i must be processed to yield information on the presence or absence of a terrain obstacle (slope). Each terrain index that is presented processes the sensor measurements in a particular manner to yield a numerical quantity which is compared to an index test number. The test of the numerical quantity is made to detect the presence of a terrain

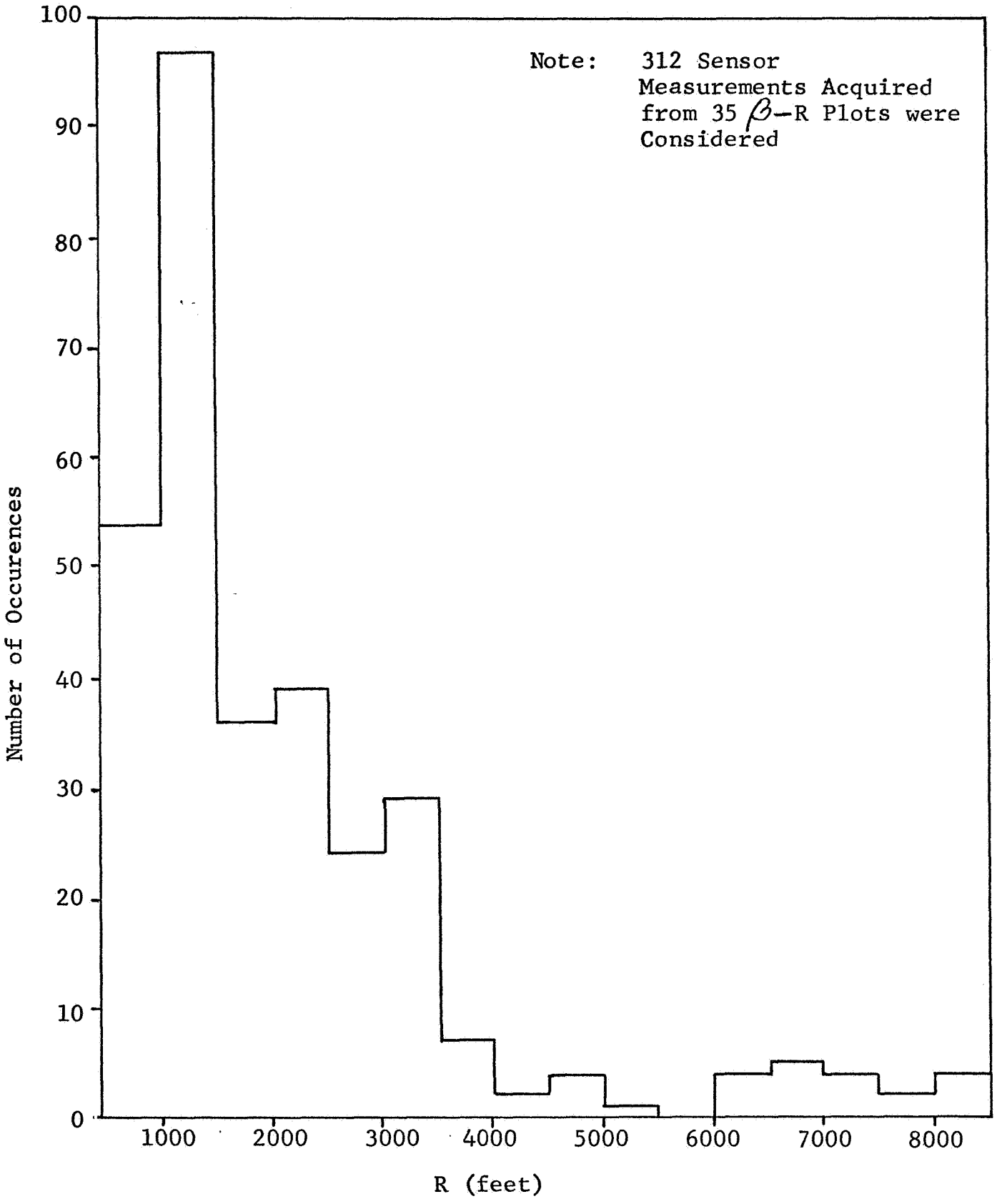

FIGURE 7. Histogram of the Distribution of Sensor Information

obstacle.

All of the terrain indices use β vs. R sensor information that can be acquired along fixed azimuth directions (θ_j). It is assumed that the sensor can acquire successive range measurements (R) along an azimuth direction for increasing values of elevation angle (β). Thus, R will be a monotone increasing function along a terrain profile in all cases of interest.

A. Slope Index

A calculation of the linear approximation to the slope along a terrain profile is made. The slope along a profile is defined as the in-path slope (S_I) and it is derived in the Appendix in terms of sensor measurements. The formula for S_I is

$$S_I = \frac{\beta_2 R_2 - \beta_1 R_1}{R_2 - R_1} \tag{3.1}$$

where the quantities β_1, R_1 and β_2, R_2 denote successive measurements of elevation angle and range for a fixed azimuth. Generally, β_2 will be equal to $\beta_1 + \Delta\beta$. The numbers "1" and "2" denote the first and second measurements of any pair of constant azimuth readings.

The slope index compares the calculated value of S_I against the index test number, T_s, by ascertaining if the inequality

$$\frac{\beta_2 R_2 - \beta_1 R_1}{R_2 - R_1} \geq T_s \tag{3.2}$$

is satisfied. If it is, then R_1 is taken as the estimated range to an obstacle along that particular azimuth, Θ_j. In the testing done, T_s was taken as tan 10°.

As the size of $\Delta\beta$ used to acquire terrain information is increased, the calculated value of S_I tends to yield a lower estimate of the true slope. In this case the linear approximation of the slope is necessarily made over a longer segment of the terrain profile. Thus, if a large value of $\Delta\beta$ is used, it may be necessary to use a lower value of T_s in order to avoid local slopes which would exceed 10 degrees.

The index would be of little merit if R_1 corresponded to a different terrain feature than R_2. In this case, the calculated value of S_I would then only represent the slope of an imaginary line connecting the two terrain features sensed. A means of overcoming this situation is to use another terrain index in conjunction with the slope index that would be applicable for this situation.

B. Gradient Index

A numerical approximation to the gradient of a terrain feature is made by varying both Θ and β for a set of measurements. The formula for the gradient calculation is developed from the magnitude of the gradient (Ref. 12) in polar coordinates where the altitude Z is described as

a function of position, $Z = Z(D, \Theta)$, to yield

$$\left| G \right| = \sqrt{\left(\frac{\partial Z}{\partial D}\right)^2 + \left(\frac{1}{D} \frac{\partial Z}{\partial \Theta}\right)^2} \qquad (3.3)$$

The first term in (3.3) can be approximated by S_I as indicated in the Appendix, calculated along the line of constant azimuth $\Theta = \Theta_j$. The second term in (3.3) can be approximated by the cross-path slope (S_c) which is derived in the Appendix in terms of three sensor measurements acquired along a pair of adjacent azimuth directions, Θ_j and Θ_{j+1}. The cross-path slope (S_c) is the slope of the terrain feature that is perpendicular to the constant azimuth profile. The square root term in (3.3) may be expanded to yield

$$\left| G \right| = S_I \left[1 + \frac{1}{2} \left(\frac{S_c}{S_I}\right)^2 - \frac{1}{4} \left(\frac{S_c}{S_I}\right)^4 + \ldots\ldots \right] \qquad (3.4)$$

provided that S_I is greater than S_c. An upper bound on $\left| G \right|$ is found by using only the first two terms of the expansion since the first term dropped is negative and dominates the error.

The gradient index compares the calculated value of $\left| G \right|$ against the index test number, T_g, by checking the validity of the inequality

$$S_I + \frac{1}{2} \frac{S_c^2}{S_I} \geq T_g \qquad (3.5)$$

If S_c is found to be greater than S_I, the square root term in (3.3) is expanded in terms of $(S_I / S_c)^2$. The

gradient index would then involve the following comparison

$$S_c + \frac{1}{2}\frac{S_I^2}{S_c} \geq T_g \qquad (3.6)$$

If either (3.5) or, if applicable, (3.6) is satisfied, then R_1 as given by (3.1), is taken as the estimated range to an obstacle along the line whose azimuth is Θ_j.

The cross-path slope (S_c) is calculated from sensor measurements made along the line $\Theta = \Theta_j$ and along the line corresponding to either $\Theta = \Theta_j + \Delta\Theta$ or $\Theta = \Theta_j - \Delta\Theta$. If $\Delta\Theta$ is large with respect to the slope variation of the terrain, the value of S_c calculated using Θ_j and $\Theta_j + \Delta\Theta$ will differ substantially from the value calculated using Θ_j and $\Theta_j - \Delta\Theta$. Thus, the effectiveness of the gradient calculation to detect the true slope of the terrain is not only a function of the size of $\Delta\Theta$, but also the choice of the adjacent azimuth direction used for the calculations.

C. Relative Altitude Index

A calculation of the relative altitude, Z, of a terrain feature is made in order to indirectly indicate the presence of a steep slope. The rationale for this calculation is that a steep slope is usually associated with a significant change in the relative altitude. The relative altitude can be calculated from one sensor measurement, using

$$Z_i = \beta_i R_i \qquad (3.7)$$

The absolute value of the relative altitude is compared with an index test number, T_r , by testing the following inequality:

$$\left| \beta_i \, R_i \right| \geq T_r \tag{3.8}$$

If (3.8) is satisfied, an obstacle is assumed to begin at the previous range measurement along that azimuth line. The value of T_r should be determined by the type of terrain that will be encountered, using either the statistical distribution of slope with Z or empirical test data.

Since this test uses an indirect measure to find a steep slope it also should be stated that it could fail to identify a steep slope (i.e., a steep slope not immediately corresponding to a significant change in Z) as an obstacle, or could label fairly safe but gently rising terrain as an obstacle.

A significant feature of this index is the simple calculations required to detect a steep slope. Thus, this index should be relatively insensitive to sensor measurement errors. It is interesting to note that this index defines an obstacle in a similar manner as Lim (Ref. 2) for a myopic robot.

D. Vertical Index

A calculation of the change in successive values of R is made to indirectly indicate the presence of a steep

slope along a terrain profile. The vertical index compares the calculated change in R against an index test number, T_v , and can be written as

$$R_2 - R_1 \leq T_v \tag{3.9}$$

If (3.9) is satisfied, R_1 is taken as the estimated range to an obstacle along the line $\Theta = \Theta_j$. The rationale for this index is the following: since an increase in β from β_1 to β_2 is associated with a change in Z, a small change in R would correspond to a steep slope, as indicated in Figure 8.

This index can be used in conjunction with the relative altitude index to partially overcome the limitation of the latter by detecting a steep slope that does not correspond to a significant change of Z. If T_v is chosen to be a fixed value, it is very effective in detecting the presence of a 10 degree slope (for example) at one particular range, say $\bar{R}$. However at ranges less than $\bar{R}$ the index is conservative since it considers slopes to be obstacles that are less than 10 degrees. Likewise, at ranges greater than $\bar{R}$, it fails to detect a 10 degree slope as an obstacle. This effect is illustrated in Table 1 where typical values of $R_2 - R_1$ are given if a 10 degree slope is to be measured (i.e., $\Delta\beta = .005$ radian) at various ranges from the vehicle.

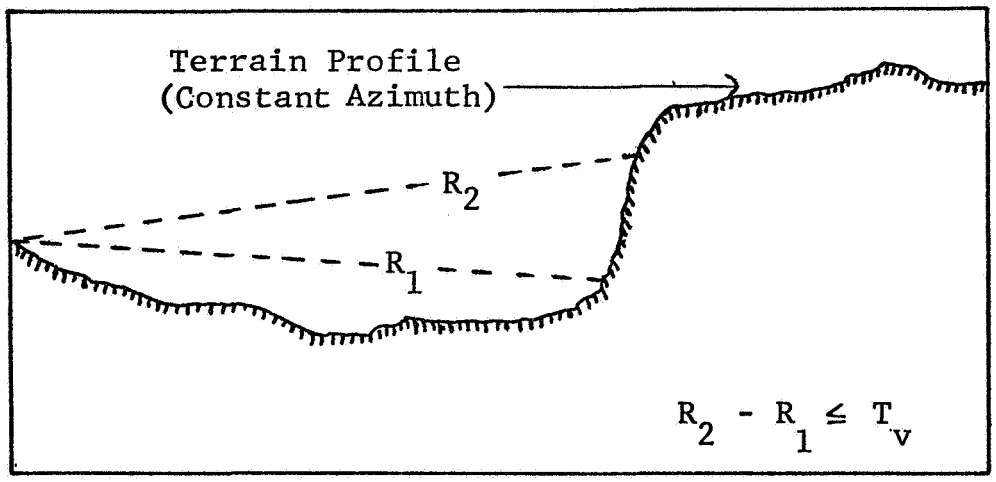

FIGURE 8. Illustration of the Vertical Index

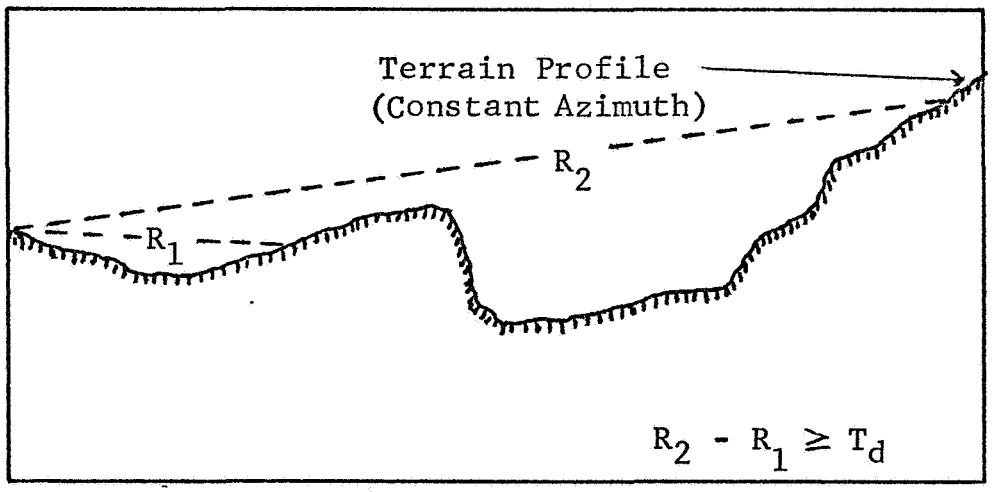

FIGURE 9. Illustration of the Discontinuity Index

TABLE 1 - Change in R for Measuring a 10° Slope

R (feet)	$R_2 - R_1$ (feet)
500	14.2
1000	28.4
2000	56.8
3000	85.2
4000	113.6

If the formula for S_I is solved for the difference $R_2 - R_1$, the resulting equation describes the variation of the range increments in terms of sensor parameters and S_I namely,

$$R_2 - R_1 = \left(\frac{\beta_2 - \beta_1}{S_I - \beta_1}\right) R_2 \qquad (3.10)$$

If T_v were defined as the right side of (3.10), this index would become just a restatement of the slope index. Thus, T_v will be chosen to be fixed.

E. Discontinuity Index

A calculation of the change in successive values of R is made to indicate the size of areas that are hidden from the vehicle for the obvious reason that these hidden areas may contain terrain obstacles.

The discontinuity index compares the calculated change in R against an index test number, T_d, and can be written as

$$R_2 - R_1 \geq T_d \qquad (3.11)$$

If (3.11) is satisfied, R_1 is taken as the estimated range to a potential obstacle along the azimith $\Theta = \Theta_j$ as indicated in Figure 9. The value of T_d was obtained by empirical data from the sample terrain.

There are difficulties in assigning a value to T_d which is used to label hidden areas as obstacles. If T_d is made too large, there would be a high probability of encountering an obstacle in the hidden area. If T_d is made too small, relatively safe terrain would be labeled as being an obstacle. As an example of the latter, if a vehicle sensed a uniform sloping terrain of 1 degree, then, for $\Delta\beta$ = .005 radians, the difference $R_2 - R_1$ would be only 100 feet at a nominal range of 1100 feet from the vehicle, but 1000 feet at a range of 3500 feet.

IV. TERRAIN MODEL GENERATION

A terrain modeling method is defined to be the repetitive application of certain terrain indices along successive azimuth directions to generate a table of azimuth values and ranges to the nearest obstacle. The following is a brief description of the operation of a modeling method: along each azimuth profile, the sensor measurements are tested until one of the indices indicates the probable presence of an obstacle. Then the range (R) to the obstacle and the corresponding value of Θ_j are stored in a table in the computer memory. If no obstacle is found along a particular azimuth direction (Θ_j), the last

R measurement and corresponding value of Θ_j are entered in this table.

Alternate modeling methods are developed that differ in the type of computing capability required and the manner used to define terrain obstacles. The modeling methods formulated and tested are listed below, with their associated terrain indices:

Method 1:	Discontinuity Index
	Vertical Index
	Relative Altitude Index
Method 2:	Discontinuity Index
	Slope Index
Method 3:	Discontinuity Index
	Gradient Index

The first method detects obstacles by indirect means and requires little computing capability. The second method essentially uses the two dimensional terrain information along an azimuth profile to define an obstacle, while Method 3 uses three dimensional terrain information. Method 3 requires more computing capability than the other methods.

The operation of the modeling methods was simulated using a WANG 370 Series Calculator (a programmable electronic desk calculator). Methods 1 and 2 were programmed with 108 and 103 operations (i.e.,add, multiply, change sign, etc.), respectively. Due to the limited program capacity, Method 3 was performed using two separate programs of 103 and 158 operations.

Storage and recall of previous sensor data was manually performed for this method.

The simulation of the methods on an electronic desk calculator demonstrated the feasibility of using these same methods with a small onboard computer. The simulation also provided a practical means of processing large amounts of sample terrain data to test the effectiveness of the methods in modeling actual terrain.

A. Comparison of Terrain Modeling Methods

Terrain models of the selected areas described in Section IIA were constructed using each of the three modeling methods presented above. The modeling methods were designed to detect the passable terrain around the vehicle by processing sensor measurements. Passable terrain is defined in terms of the distance that a vehicle can travel in a given direction before encountering a terrain obstacle. In this study, the maximum possible range was limited to 4000 feet, and a slope in excess of 10^{o} was considered as an obstacle. Sensor measurements were acquired in increments of .005 radian (.3 degree) in elevation angle ($\Delta\beta$) and 5^{o} degrees in azimuth angle ($\Delta\Theta$) to form a common basis to compare the individual modeling methods. The following index test numbers were used: T_s = tan 10^{o}, T_g = tan 10^{o}, T_r = 40 feet, T_v = 25 feet, and T_d = 1000 feet.

The effectiveness of a method to model terrain was evaluated by considering the following three factors for each of the three areas:

1. The percentage of the passable terrain detected. It is noted that terrain slopes of 10^{o} or more contained within a 1^{o} sector of terrain were considered as local terrain irregularities and not as terrain obstacles.
2. The maximum range error computed. A range error is defined as the difference between the computed range (R) and the actual range to the first obstacle along a terrain profile. Only a computed R which is an overestimate of the range to the obstacle is considered.
3. The percentage of terrain profiles along which a range error was computed.

The results of these tests are summarized below.

Area 1: Method 1 found 39.7% of the passable terrain. The passable terrain that was not detected was the result of: 1). passable terrain was hidden from the vehicle's view, 2). some of the significant changes in Z did not correspond to a terrain obstacle. Due to the convex shape of the terrain profile along two azimuth directions, large portions of passable terrain were hidden from the vehicle and thus were considered as obstacles. The existence of this hidden area also

effected the results obtained with the other two methods. A range error was found along 37% of the terrain profiles. The maximum range error was 150 feet which occurred for an actual obstacle at a range of 3250 feet. This range error was generally due to either a steep slope that did not correspond to a significant change in Z (i.e., T_r) or a change in R that was less than T_v.

Methods 2 and 3 found 61.9% of the passable terrain. A range error was found along 25% of the terrain profiles. The maximum range error was 50 feet which occurred for an actual obstacle at a range of 3250 feet. The range errors were due to the value of $\Delta\beta$ not being small enough to detect a narrow band (50 feet) of steep slope at a range of 3250 feet.

Area 2: All three methods found only 9.2% of the passable area. In this sector, relatively large areas of terrain near the assumed vehicle location were hidden from view. The discontinuity index was the primary means of detecting obstacles in this region. No range errors were found in this sector. This was primarily because empirical data was used in selecting the value of T_d.

Area 3: There was a high percentage of passable terrain detected using all the methods since the assumed vehicle location offered a fairly good view of the terrain in the area. Method 1 found 61.5% of the passable terrain. The relative altitude index was effective in

detecting the presence of steep slopes because of the high correlation between the change in altitude and a steep slope. A range error was found along 27% of the terrain profiles. The maximum range error was 90 feet which occurred for an actual obstacle at a range of 1110 feet. The range error was due to the indirect means used to estimate the presence of a steep slope.

Method 2 found 80.4% of the passable terrain. A range error was found along 45% of the terrain profiles. The maximum range error was 390 feet which occurred for an actual obstacle at a range of 1000 feet. The large frequency and size of range errors was due to the fact that the slope along many of the terrain profiles was much less than the actual slope of the terrain, i.e., the cross-path slope was significant.

Method 3 found only 54% of the passable terrain. The relatively low percentage of passable terrain detected was due to the "large" size of $\Delta\theta$ in relation to the size of the slope irregularities of the terrain. Both of the alternative azimuth directions were used in the gradient calculation. The most conservative estimate for the range to an obstacle was used for the terrain model. A range error was found along only 9% of the terrain profiles. The maximum range error was 70 feet which occurred for an actual obstacle at a range of 2800 feet. An

improvement in the range accuracy could be expected if a smaller increment in azimuth were used to acquire sensor measurements.

Even though the effectiveness and applicability of each method varied with the terrain modeled, the following properties of the modeling methods were observed as a result of the above comparison.

Method 1 detects a relatively small amount of passable terrain with modest size range errors. The effectiveness of this method is primarily limited by the indirect means used to detect the presence of a steep slope.

Method 2 detects the highest percentage of passable terrain but it results in relatively significant range errors if there is a significant cross-path slope present.

Method 3 detects a modest percentage of the passable terrain with the size of $\Delta\Theta$ used, but it results in the lowest range error of any method. The effectiveness of this method should be significantly increased if a smaller increment in azimuth angle was used.

B. Terrain Sensor Measurement Requirements

The effectiveness of the terrain modeling method depends on the characteristics of the terrain sensor available. A summary is given of some of the sensor measurement characteristics necessary to use the modeling

techniques developed.

1. Range

A terrain sensor was assumed to be available that could provide range measurements for distances up to 4000 feet from the vehicle. The upper limit of 4000 feet was taken as the maximum range at which the modeling methods could be effectively applied to the sample terrain since sufficient terrain (sensor) information was not available at ranges greater than 4000 feet, as previously illustrated in Figure 7. There are two explanations why terrain information is more difficult to acquire as larger values of R are considered. First, terrain features relatively near the vehicle tend to obstruct line-of-sight measurements of terrain features relatively far from the vehicle. Second, the 1/R factor in the β vs. Z relationship (2.2) tends to enlarge the minimum magnitude of Z that can be measured as R is increased, i.e., for a fixed value of β.

If the sensor range measurements (R) are measured with some inaccuracy, the effectiveness of a modeling method will be reduced corresponding to the type of calculations that are made with these range measurements. As an example, the slope index requires differencing, multiplication and division operations, while the relative altitude index requires only the multiplication operation. The variations in the calculated values of the in-path

slope, e.g., S_I = tan 10° = .176, and the relative altitude, e.g., Z = 40 feet for deviations of ± 10 feet in the range measurements are shown in Table 2.

TABLE 2. Effect of Range Measurement Errors of ± 10 Feet on Calculated Values of Z and S_I (β_1= 0 and β_2= .01 radian)

Nominal Range (feet)	Calculated Z (feet)		Calculated S_I	
	Low	High	Low	High
1000	39.6	40.4	.130	.276
2000	39.8	40.2	.152	.224
3000	39.9	40.1	.156	.200
4000	39.9	40.1	.162	.194

The maximum error in evaluating Z was 1% while the maximum error in evaluating S_I was 36%. Thus, Modeling Method 1 which includes the relative altitude index is less sensitive to range measurement errors than Method 2, which includes the slope index. It is noted that tan 10° and 40 feet were the values of T_s and T_v used in the simulation of the methods above to estimate the presence of an obstacle.

2. Elevation Angle Increment

The size of the β increment used in acquiring sensor data directly affected the performance of the terrain modeling techniques. In Table 3, the percentage of the total passable terrain detected when the results for areas 1,2, and 3 are combined is tabulated as a function

of the increment $\Delta\beta$ used to acquire sensor data.

TABLE 3. Percentage of Passable Terrain Detected as a Function of $\Delta\beta$

$\Delta\beta$ (radians)	Method 1 (% passable terrain)	Method 2 (% passable terrain)
.005	31.7	44.5
.010	32.1	37.3
.015	17.8	21.0
.020	9.8	11.6
.025	8.2	9.9
.030	7.3	8.7

There was a general decrease in the percentage of passable terrain detected when larger increments of β were used. This decrease in percentage was related to the amount of information that was available to the terrain modeling method. In Table 4, the average number of sensor measurements available was tabulated as a function of the size of $\Delta\beta$, i.e., for a fixed azimuth direction.

TABLE 4. Average Frequency of Sensor Measurements as a Function of $\Delta\beta$

Increment $\Delta\beta$ (radians)	Average Number of Sensor Measurements
.005	8.2
.010	4.2
.015	3.0
.020	2.4
.025	2.0
.030	1.8

It would be possible to increase the percentage of passable terrain detected, if the index test numbers were optimized for the value of $\Delta\beta$ used. For example, the slope calculation of S_I yielded a lower approximation to the true slope if $\Delta\beta$ was large. Thus, a smaller value of T_s should be chosen to account for the "cruder" slope approximation.

3. Azimuth Angle Increment

The size of the Θ increment used to acquire the sensor data should be related to the general characteristics of the terrain to be modeled. The increment in Θ must be small enough to detect significant information about major terrain features that would be typically encountered.

In general, the effectiveness of a modeling method decreased as the size of $\Delta\Theta$ was increased. This trend was observed from the simulation work when the percentage of total passable terrain was seen to decrease as $\Delta\Theta$ was increased, refer to Table 5.

TABLE 5. Percentage of Passable Terrain Detected as a Function of $\Delta\Theta$ ($\Delta\beta$ = .005 radian)

$\Delta\Theta$ (degrees)	Method 1 % passable terrain	Method 2 % passable terrain
5	31.7	44.5
10	21.7	26.7

V. DISCUSSION

Three terrain modeling methods were developed in this report for an exploratory vehicle's long range path selection. The modeling method selected for a particular guidance system would depend upon the trade-offs made between the modeling effectiveness desired and the computer and sensor capabilities available.

The performance of the methods was simulated on a sample terrain. The modeling methods could be adapted for terrain dissimilar to the sample terrain by proper choice of the terrain index test numbers.

The main restriction on the terrain modeling effectiveness was the line-of-sight measurement requirement. If the effectiveness of a method was not acceptable, provisions might have to be made to supply the vehicle with additional terrain information. Possibilities would include a second sensor located on a vertical extension of the vehicle which could be raised when the vehicle was stopped or perhaps data sent from a satellite orbiting overhead.

There were several difficulties in interpreting discrete line-of-sight sensor measurements. For example, consider the two sensor measurements illustrated in the terrain profiles shown in Figures 10A and 10B. The same sensor measurements can be obtained from quite different terrain configurations. Thus, the modeling method must be designed to make good

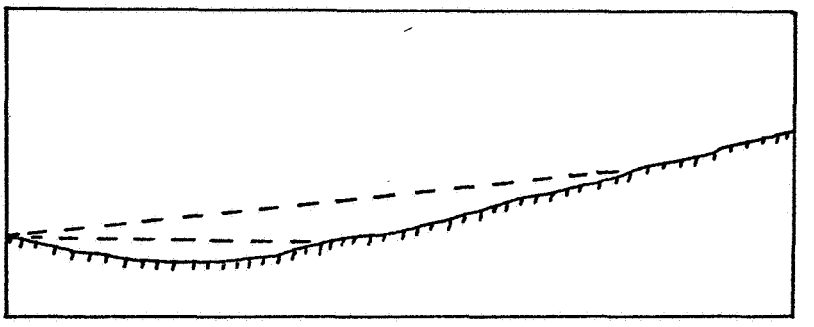

A. Continuous Slope Terrain Profile

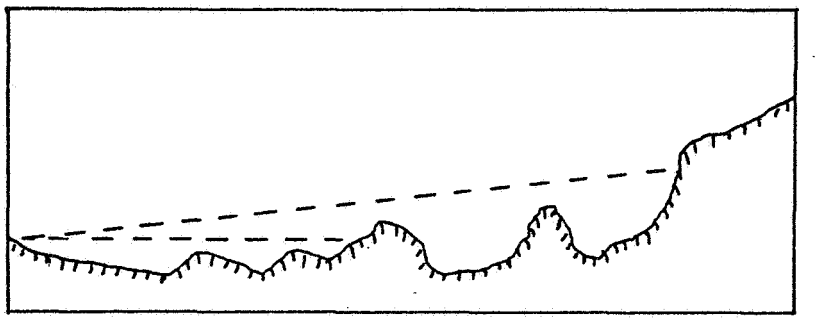

B. Hidden Obstacle Terrain Profile

FIGURE 10. Possible Terrain Configurations Given the Same Two Discrete Sensor Measurements

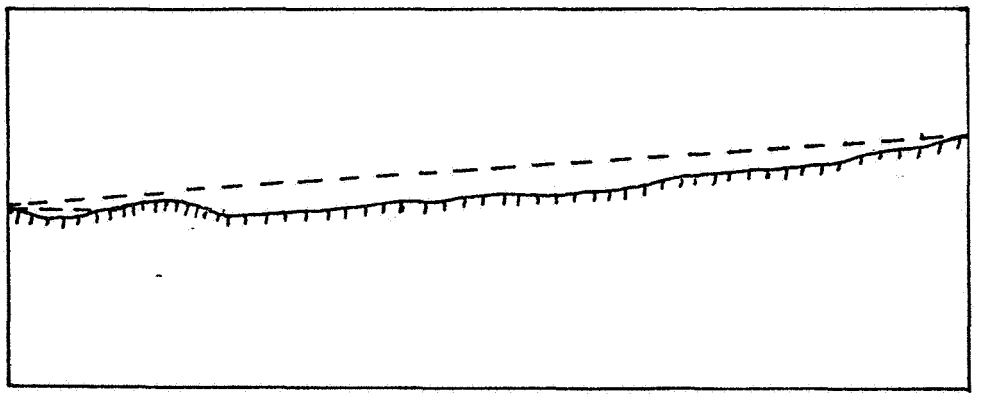

FIGURE 11. Illustration of Hidden Passable Terrain

"guesses" on the terrain configuration, and, due to the nature of the mission, these guesses should be on the conservative side.

A typical situation encountered in the simulation work was the occurrence of passable terrain which was hidden from the view of the vehicle by a terrain configuration near the vehicle's location. An example of such terrain is shown in Figure 11. The terrain presents no actual obstacle but the vehicle could not "see" it from the vehicle location shown. If the hidden area was large enough so that $R_2 - R_1 \geq T_d$, then the modeling method would designate the area as an obstacle region. A possible means to overcome this situation would be to form a terrain model with two types of unsatisfactory terrain, namely, confirmed obstacles, obtained by using the slope index, vertical index, etc., and potential obstacles, obtained by using the discontinuity index. Then, if the vehicle could not find a suitable path from its original vantage point, it might move in small increments towards a potential obstacle in the hope that it would be able to get to a better vantage point.

Even though the modeling techniques presented in this report were designed for long range terrain modeling, it would seem that they could be adapted for short range terrain modeling. If it is desired to extend these techniques for this case, certain factors should be considered:

a. The index test numbers should be chosen specifically

for the range of terrain to be modeled.

b. Additional indices may be required to account for obstacles peculiar to short range modeling, e.g., size and spacing of vertical obstacles.

c. Small angle approximations that had been used to simplify the numerical calculations may not be valid for short range modeling, in which case additional computing requirements would be necessary to evaluate the trigonometric functions.

VI. CONCLUSION

The problem considered in this report is the mathematical modeling of major terrain features using measurements acquired at a single terrain location, to be used in a self-contained surface vehicle guidance system. The terrain modeling problem was posed for long-range vehicle guidance, and was conceived to consist of three function parts: terrain data acquisition, terrain data processing, and terrain model generation.

In Section II, terrain sensor measurements which must provide the inputs to any long range terrain modeling system were simulated by using a sample terrain. Basic properties of the terrain sensor measurements were deduced from the empirical data compiled from the sample terrain.

In Section III, specific methods of processing sensor measurements were developed in the form of terrain indices. The terrain indices would enable the vehicle to detect the

presence of an obstacle to travel by processing the acquired sensor measurements. A number of indices were developed to provide flexibility in designing a terrain modeling system. The indices vary in the complexity of the calculations that must be performed and the accuracy that can be expected in detecting an obstacle.

In Section IV, complete terrain modeling methods were developed using various combinations of the terrain indices described in the previous section. These methods were compared with respect to their terrain modeling effectiveness and their associated computer and sensor requirements.

This investigation has provided three contributions in the area of long range vehicle guidance for an exploratory surface vehicle. First, it has developed methods to perform long range terrain modeling with only modest computing requirements. Second, it has developed general terrain sensing and computer requirements necessary to perform long range terrain modeling for a selected sample terrain. Third, it has provided general techniques to formulate terrain modeling methods for varied terrain situations.

Future work in terrain modeling could include: 1). the testing of the modeling methods on other representative terrains to optimize the performance of the methods, 2). extending the techniques developed to the problem of short range terrain modeling for surface vehicle guidance.

APPENDIX

Derivation of the Slope Formulas Required for the Slope and Gradient Indices

1. In-Path Slope

The In-Path Slope (S_I) of a terrain segment is defined as the linear approximation to the slope of a terrain segment in the direction of a constant azimuth terrain profile, and it is expressed as the tangent of the corresponding slope angle, as indicated in Figure 12. It can be approximated by dividing the change in altitude by the corresponding change in the horizontal distance,

$$S_I = \frac{\Delta Z}{\Delta D} \tag{A1}$$

If the altitude Z is described as a function of position in polar coordinates, $Z = Z(D, \Theta)$ with the vehicle at the origin, then S_I can be interpreted as the numerical approximation to the partial derivitive of Z with respect to D,

$$\frac{\partial Z}{\partial D} \backsimeq \frac{\Delta Z}{\Delta D} \tag{A2}$$

This approximation becomes exact in the limit as ΔD approaches zero.

The in-path slope can be written in terms of two successive sensor measurements acquired along a fixed azimuth direction. The quantities R_1 and R_2 denote the corresponding range measurements for the elevation angles β_1 and β_2

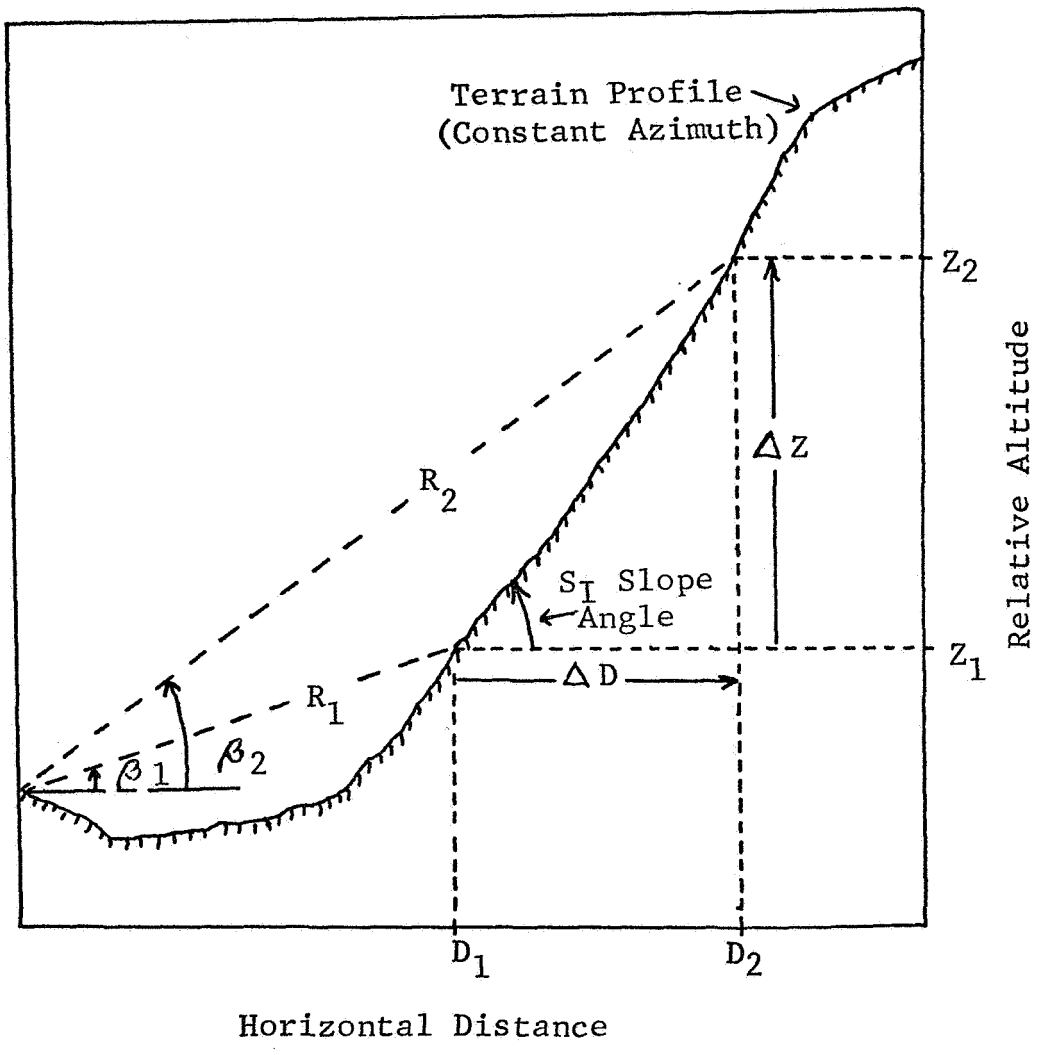

FIGURE 12. Illustration of the S_I Calculation

($\beta_2 = \beta_1 + \Delta\beta$). S_I can be rewritten in terms of the two sensor measurements as

$$S_I = \frac{R_2 \sin\beta_2 - R_1 \sin\beta_1}{R_2 \cos\beta_2 - R_1 \cos\beta_1} \qquad \text{(A3)}$$

Since only small values of elevation angle will be used (see Section IIC), the following approximations are made: $\sin\beta \simeq \beta$ and $\cos\beta \simeq 1$. Inserting these approximations into equation (A3), S_I becomes

$$S_I = \frac{R_2\beta_2 - R_1\beta_1}{R_2 - R_1} \qquad \text{(A4)}$$

which is in a form that may be easily implemented on a small computer.

2. Cross-Path Slope

The Cross-Path Slope (S_c) of a terrain segment is defined as the linear approximation to the slope of a terrain segment in a direction perpendicular to a constant azimuth terrain profile, and it is expressed as the tangent of the corresponding slope angle as indicated in Figure 13. It can be approximated by dividing the change in altitude by the corresponding change in the horizontal distance (arc length),

$$S_c = \frac{\Delta Z}{D\Delta\Theta} \qquad \text{(A5)}$$

If the altitude Z is described as a function of position in polar coordinates, $Z = Z(D, \Theta)$ with the vehicle at the origin, then S_c may be interpreted as the numerical approximation to the partial derivative of Z with respect to Θ divided by D,

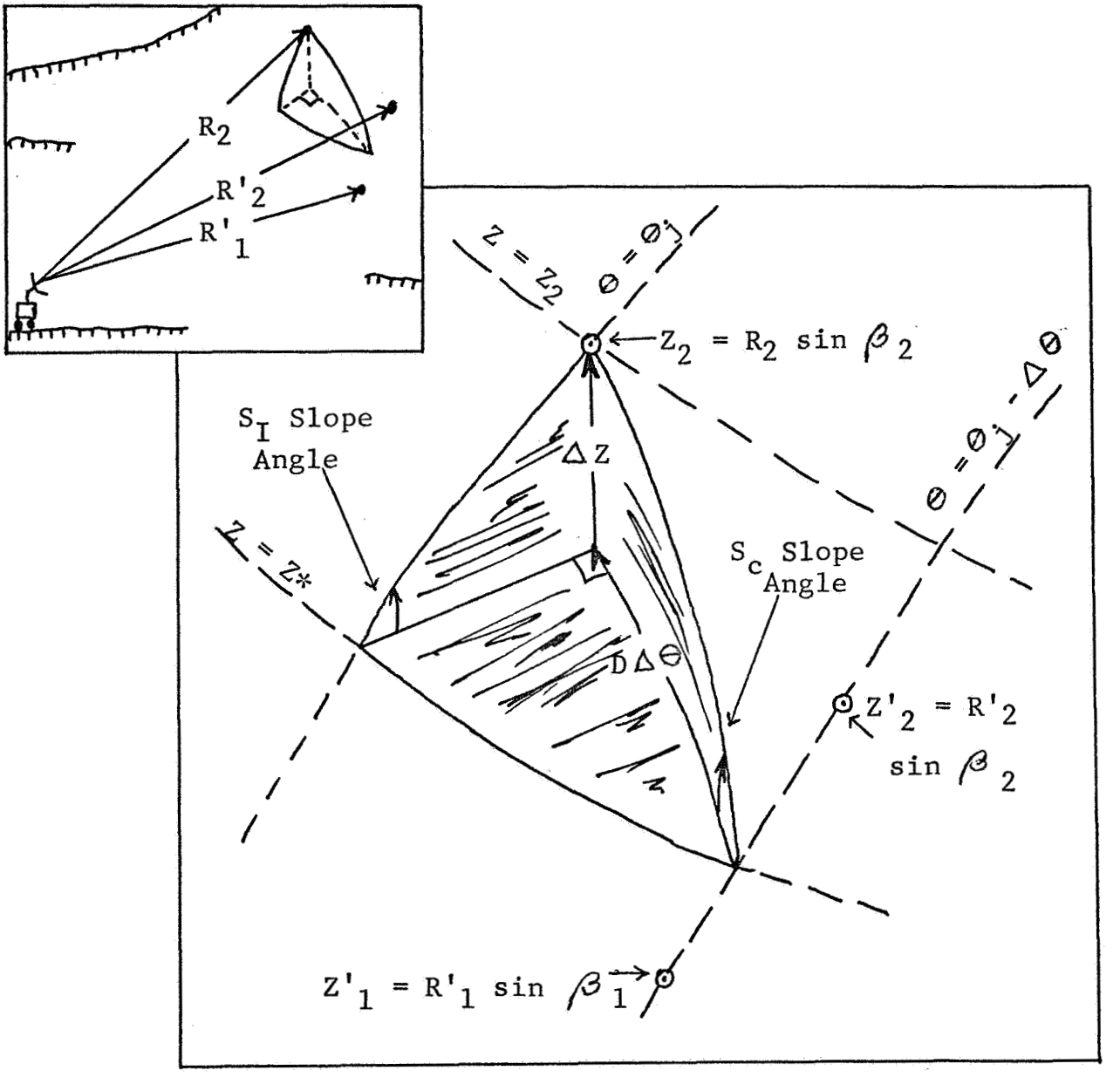

FIGURE 13. Illustration of the S_c Calculation

$$\frac{\partial Z}{D\partial\theta} \simeq \frac{\Delta Z}{D\Delta\theta} \tag{A6}$$

where the approximation becomes exact in the limit as $\Delta\theta$ approaches zero.

The formula for S_c may be written as

$$S_c = \frac{(Z_2 - Z^*)}{D_2 \Delta\theta} \tag{A7}$$

where Z_2 and Z^* are discrete points on the terrain each at a distance D_2 from the vehicle. If the point Z_2 can be measured directly from sensor data, i.e., $Z_2 = R_2 \sin\beta_2$, at a distance D_2, i.e., $D_2 = R_2 \cos\beta_2$, then, the altitude Z^* cannot be measured directly from sensor measurements since only θ and β can be specified by the vehicle's terrain sensor (see section IIB). The altitude Z^* can be indirectly measured by first computing the in-path slope S_I' from two successive sensor measurements R_1', β_1, and R'_2, β_2 acquired along the azimuth line $\theta = \theta_j - \Delta\theta$. S'_I will be an in-path slope approximation in the vicinity of Z^*, since β_2 is held fixed to acquire R_2 and R'_2 and β_1 equals $\beta_2 - \Delta\beta$. The slope S'_I can be computed from these sensor measurements using equation (A3) so that

$$S'_I = \frac{R'_2 \sin\beta_2 - R'_1 \sin\beta_1}{R'_2 \cos\beta_2 - R'_1 \cos\beta_1} \tag{A8}$$

which may also be written in terms of Z* as

$$S'_I = \frac{R'_2 \sin \beta_2 - Z^*}{R'_2 \cos \beta_2 - R_2 \cos \beta_2} \qquad \text{(A9)}$$

This equation can be solved for Z* in terms of sensor measurements. If the indicated substitutions for Z_2, Z* and D_2 are inserted into (A7) and the small angle approximations for $\cos\beta$ and $\sin\beta$ are again used, S_c can be written as

$$S_c = \frac{(\beta_2 - S'_I)(R_2 - R'_2)}{R_2 \Delta\theta} \qquad \text{(A10)}$$

When either an in-path or cross-path slope calculation is made, the sensor measurements needed for the calculation must be acquired from the same terrain feature in order to obtain valid slope approximations. A processing system can estimate the applicability of a slope calculation for a given set of sensor measurements by testing the size of the range differencing factor (e.g., $R_2 - R'_2$) that is required in the slope calculation.

REFERENCES

1. Lallman, F.J., "Automatic Path Selection", Technical Report V of Progress Report, "Analysis and Design of a Capsule Landing System and Surface Vehicle Control System for Mars Exploration", by P.K. Lashmet, et. al., NASA Grant NGR 33-018-091, Rensselaer Polytechnic Institute, June 1968.

2. Lim, L.Y., "A Pathfinding Algorithm for a Myopic Robot," T.R. 32-1288, Jet Propulsion Laboratory, Pasadena, Calif., August 1968.

3. Shamberger, J.H., "Mobility Environmental Research Study a Quantitative Method for Describing Terrain for Ground Mobility", Vol. 1, TR No. 3-726, U.S. Army Engineer Waterways Experiment Station, Corp of Engineers, Vicksburg, Mississippi, May 1968.

4. Dornbusch, W.K., Jr., "Mobility Environmental Research Study a Quantitative Method for Describing Terrain for Ground Mobility", Vol. III, TR No. 3-726, U.S. Army Engineer Waterways Experiment Station, Corp of Engineers, Vicksburg, Mississippi, September 1967.

5. Dornbusch, W.K., Jr., "Mobility Environmental Research Study a Quantitative Method for Describing Terrain for Ground Mobility", Vol. VII, TR No. 3-726, U.S. Army Engineer Waterways Experiment Station, Corp of Engineers, Vicksburg, Mississippi, April 1968.

6. deWys, J.N., "Martian Scientific Model", PD 606-1, Jet Propulsion Laboratory, Pasadena, Calif., 1968.

7. Crawford, J.W., "The Vehicle", Chapter I of Progress Report, "Control Components for an Unmanned Lunar Roving Vehicle", NASA Grant NSR 33-010-055, Cornell University, June 1968.

8. S. Kaufman, et.al., "Off-Road Mobility Research", Cornell Aeronautical Laboratory, Inc., TR No. VJ-2330-G-2, September 1967.

9. Dugoff, H., "Vehicle Egress From a Stream-A Mathematical Model", Journal of Terramechanics," 1967, pp. 17-29.

10. Bartlett, G.E., "On the Prediction of Off-Road Vehicle System Mobility", International Automotive Engineering Congress, Detroit, Michigan, January 1969.

11. Map of Nassau Quadrangle, New York-Rensselaer Co., 7.5 Minute Series (Topographic), SE/4 Troy 15 Quadrangle, prepared by U.S. Geological Survey, 1953.

12. Kaplan, W., "Advanced Calculus," Addison-Wesby Publishing Co., Reading, Massachusetts, 1952.